Generating symmetry and symmetry breaking in sand-bubbler patterns

Hendrik Richter

HTWK Leipzig University of Applied Sciences, Faculty of Engineering
Department of Electrical Engineering and Information Technology, Postfach 301166, D–04251 Leipzig, Germany
hendrik.richter@htwk-leipzig.de

Abstract

We study creating and breaking symmetry in digitally generated artificial-life-based visual art. Therefore, an artificial swarm-based pattern-making system is used as a test bed. The patterns are generated algorithmically by emulating the collective feeding behavior of sand-bubbler crabs. Our focus is on analyzing concepts and templates for incorporating symmetry and broken symmetry into the creation process of bioinspired art. All four types of two-dimensional symmetry defined by isometric maps are used to create images. Apart from treating geometric symmetry, we also consider color as an object of symmetric transformations. Color symmetry is realized as a color permutation consistent with the isometric maps. Therefore, color permutation groups have been designed which utilize mappings on a color wheel.

Introduction

Different types of collective animal behavior occurring, for instance, in swarms, flocks and colonies are particularly interesting as they might show algorithmic ideas and templates potentially helpful as an inspiration for artificial-life-based art. Examples are ant- and ant-colony-inspired visual art (Greenfield and Machado, 2015; Urbano, 2011), but also the pattern-making of insects (Abbood et al., 2017), schools of fishes and flocks of birds (Jacob et al, 2007; Romero and Machado, 2008). Another recent example is sand-bubbler patterns (Richter, 2018). These patterns are starting point for an artistic interpretation of symmetry and symmetry breaking.

It seems to be curious that symmetry is an important property not only of aesthetically pleasing objects, but also of living organisms. Consequently, symmetry has been studied extensively in art and biology (and sciences in general) (Thompson, 1942; Weyl, 1952; Shubnikov and Koptsik, 1974; Grünbaum et al., 1986; Rosen, 1995; Conway et al., 2008; Ball, 2009; Rosen, 2009; al-Rifaie et al., 2017; Schattschneider, 2017). Consider the transformational potential from biology to artificial life as a departure point for artistic reflection (Whitelaw, 2004; Boden, 2015; Galanter, 2016). Thus, it would be desirable for the generating mechanisms of artificial-life-based art to address different aspects and meanings of symmetry from both a conceptual and a computational point of view. In this paper we take up this idea and consider generating visual art with pre-designed and tuneable degrees of symmetry. This is based on the following understanding of the essence of symmetry. Symmetry implies that between the point sets forming the geometric objects of an image, there are mappings preserving certain properties of these point sets. These properties may be associated with the spatial arrangement of the points within a set, but also with the color of the points. In other words, parts of a symmetric image resemble each other in some way or another.

Although symmetry of two-dimensional geometric objects can be easily defined mathematically by isometric maps, generating interesting symmetry in art is not trivial. Art objects that strictly adhere to mathematical definitions of symmetry may sometimes appear "overdesigned" from a human point of perception. A related problem is that symmetry in a strict mathematical sense is a binary concept. Either there is symmetry and the objects in an image obey an isometric map, or there is not. However, human artists creating works that are praised for handling subtle effects of symmetry often experiment with symmetries that are slightly (or even substantially) perturbed (Adanova and Tari, 2016; Bier, 2005; Molnar and Molar, 1986; Schattschneider, 2004). Such perturbations can be seen as symmetry breaking. From a rather abstract point of view, symmetry breaking is not meaning that the symmetry is completely absent or that there is asymmetry, but rather that some aspects of the symmetry are gone. Hence, symmetry breaking is a particularly powerful concept if it is seen as a process that plays with our expectations of symmetry. Thus, symmetry breaking needs the context of us perceiving (or at least presuming) an intact symmetry. Put differently, if before symmetry breaking there was one kind of symmetry, then a broken symmetry implies another kind of, but somehow "lesser" symmetry.

Recently, an algorithmic framework has been proposed to generate bioinspired visual art, which is based on the collective feeding behavior of sand-bubbler crabs (Richter, 2018).

In nature, these patterns consist of sand-balls. In the images inspired by nature, the patterns consist of pellets with a given color (and possibly texture). This paper deals with employing artificial sand-bubbler patterns for studying algorithmic generation and computational evaluation of symmetry and symmetry breaking. We may generate symmetry by applying to the patterns any of the four types of isometric symmetry in two-dimensional objects (e.g. (Martin, 1982; Liu et al., 2010)): (i) reflection, (ii) rotation, (iii) translation, and (iv) glide reflection.

To have images with broken symmetry we remove (or render invisible) a fraction of the pellets building the patterns. This interpretation is based on ideas proposed by Molnar and Molar (1986) that symmetry breaking in visual objects can be realized by moving or removing building blocks of the visual representation. A main advantage of such an interpretation is that by fixing a fraction of pellets and removing the amount of pellets thus allowed at random, the degree of symmetry breaking can be almost continuously scaled. If the fraction is zero, symmetry is completely intact, any fraction between zero and one breaks the symmetry to that degree, and if the fraction is equal to one, symmetry is entirely absent. We use such a scaling to pre-design and tune degrees of symmetry in sand-bubbler patterns.

As the sand-bubbler patterns have a given color, it appears interesting to consider also color as a property that may undergo symmetry transformations. This is known as color symmetry (Schwarzenberger, 1984; Senecha, 1983, 1988). There are some works on creating patterns using color symmetry, for instance Dunham (2010); Ouyang et al. (2012); Thomas (2012), and a substantial amount of the visual art of M. C. Escher uses color symmetry in some way or another (Adanova and Tari, 2016; Coxeter, 1986; Schattschneider, 2004, 2017), but there is a (somehow surprising) lack of applications in the domain of artificial-life-based and generative art. The visual and numerical results reported in this paper explicitly address the topic and deal with color symmetry in generative visual art. In visual art color symmetry is a permutation of the patterns' colors which is consistent with the symmetry of the geometric objects of the image. It can be realized by a mapping on a color wheel. Color symmetry breaking, in turn, is an (intentional or random) perturbation of the color permutation.

The paper is organized as follows. In the next section the generation of sand-bubbler patterns is briefly recalled, see also Richter (2018) for algorithmic details and biological background. It is also discussed how generating and breaking symmetry can be achieved for these patterns. This is shown for both the geometric symmetry of the patterns and the color symmetry. Following this, computational experiments and results are presented. Examples of sand-bubbler art are presented and a computational symmetry measures is tested to identify different aspects of symmetry. It is shown that the computational symmetry measure is able to identify different types of symmetry and symmetry breaking in the images. Concluding remarks end the paper with a summary of the findings and a discussion about future work.

Creating and breaking symmetry in sand-bubbler patterns

Pattern symmetry

Sand-bubblers are tiny crabs living on tropical beaches. They create remarkable patterns in the sand as part of their collective feeding behavior. According to, and adopting, the language of biological field work, these patterns consist of sand balls, called pellets, that are placed along lines, called trenches, which radiate from a center point, called burrow. Recently, it was proposed to let this behavior inspire an algorithmic framework for generating visual art. In this paper we use this framework for experimenting with symmetry and symmetry breaking, and briefly recall how the patterns are generated; see Richter (2018) for a detailed discussion about the biological background and how the feeding behavior of sand-bubbler crabs can be captured by an algorithmic description.

A sand-bubbler pattern can be described by the pellets it contains. We give every pellet a location $(x_{ijk}, y_{ijk})^T$ in a two-dimensional (x, y)-plane. The index (ijk) identifies the k–th pellet ($k = 1, 2, 3, \ldots, K_{ij}$) belonging to the j–th trench ($j = 1, 2, 3, \ldots, J_i$) of the i–th burrow ($i = 1, 2, 3, \ldots, I$). A pellet location can be computed by

$$\begin{pmatrix} x_{ijk} \\ y_{ijk} \end{pmatrix} = \begin{pmatrix} x_i + r_k \cdot \cos(\theta_j) \\ y_i + r_k \cdot \sin(\theta_j) \end{pmatrix} + \begin{pmatrix} \mathcal{N}(\mu_{ijk}, \sigma^2_{ijk}) \\ \mathcal{N}(\mu_{ijk}, \sigma^2_{ijk}) \end{pmatrix}, \tag{1}$$

where $(x_i, y_i)^T$ are the coordinates of the i–th burrow, θ_j is the trench angle of the j–th trench, r_k is the radial coordinate of the k–th pellet, and $\mathcal{N}(\mu_{ijk}, \sigma^2_{ijk})$ are realizations of a random variable normally distributed with mean μ_{ijk} and variance σ^2_{ijk}. For each burrow, we need to specify the maximum number of pellets K_{ij} for a given i and j; the same applies to the maximum number of trenches J_i.

For two-dimensional objects represented in an Euclidean space, there are four types of isometric symmetry (e.g. Martin (1982); Liu et al. (2010)): (i) reflection, (ii) rotation, (iii) translation, and (iv) glide reflection. For a sand-bubbler pattern specified by Eq. (1), we define n an integer and $(\Delta x, \Delta y)^T$ a vector of some real numbers, compute $\varrho = \sqrt{x^2_{ijk} + y^2_{ijk}}$, and obtain (left-right) reflection, rotation, translation, and (up-down) glide reflection by

$$(x_{ijk}, y_{ijk})^T \rightarrow (-x_{ijk}, y_{ijk})^T \tag{2}$$

$$(x_{ijk}, y_{ijk})^T \rightarrow (\varrho \cos(2\pi/n), \varrho \sin(2\pi/n))^T \tag{3}$$

$$(x_{ijk}, y_{ijk})^T \rightarrow (x_{ijk} + \Delta x, y_{ijk} + \Delta y)^T \tag{4}$$

$$(x_{ijk}, y_{ijk})^T \rightarrow (x_{ijk} + \Delta x, -y_{ijk})^T, \tag{5}$$

respectively. For reflection (2) and rotation (3), there are invariant points with the reflection axis $x = 0$ and the rotation center point $(x, y)^T = (0, 0)^T$, while for translation (4) and glide reflection (5), no point of the pattern remains invariant. Basically, the definitions (2)-(5) of two-dimensional isometric symmetry relate to points $(x_{ijk}, y_{ijk})^T$ representing pellets, but may also apply to point sets representing trenches, burrows or whole patterns. In this paper we consider symmetry only to act on whole burrows. For designing the visual effect that not all burrows share the same symmetry center (for rotation) or symmetry line (for reflection and in some sense also for glide reflection), it is possible to combine rotation, reflection or glide reflection with a subsequent translation. For instance, rotation (3) followed by translation (4) yields rotation center points at any $(\Delta x, \Delta y)^T$.

As important as symmetry is for aesthetically pleasing objects, it is also known that subtle beauty in nature and art is sometimes connected with symmetry that is a little less than completely perfect. For instance, in nature symmetry surely is a major organizational principle, but is rarely achieved in a strict mathematical sense. The same applies to art. See, as an example, the discussion about oriental carpets, embroideries, tilings, and ornaments (Bier, 2001, 2005; Grünbaum et al., 1986).

Such slight imperfections of symmetry fall into an intermediate state between complete symmetry and absence from any symmetry and can be related to symmetry breaking. It has been suggested by Molnar and Molar (1986) that in visual art symmetry breaking can be achieved by moving and/or removing building blocks of the visual representation. The main intention of such a moving and/or removing of visual structures is to disturb the symmetry without lastingly destroying it. This is in line with the observation that symmetry breaking in textile art (for instance oriental carpets and embroideries) can be created by intentionally or randomly inserting irregularities and perturbations, resulting in a (more or less close) approximation of symmetry (Bier, 2001, 2005).

From a computational point of view, and applied to the sand-bubbler patterns as defined by Eq. (1), this interpretation of symmetry breaking has an interesting property. By fixing a fraction of pellets and removing these pellets, the degree of symmetry breaking can be almost continuously scaled. Thus, symmetry and symmetry breaking can be predesigned and tuned, which is opening up settings for computational experiments. For generating images and evaluating them using a computational measure, we employ and analyze a parameter governing symmetry and symmetry breaking: the symmetry breaking rate σ_{break}. It describes how many of the pellets of a pattern are removed (or not visible) due to symmetry breaking. If $\sigma_{break} = 0$, symmetry is completely intact, any value $0 < \sigma_{break} < 1$ breaks the symmetry to that degree, and if $\sigma_{break} = 1$, symmetry is entirely absent. As there are in total $I_\Sigma = \sum_{i=1}^{I} \sum_{j=1}^{J_i} K_{ij}$ pellets belonging to a pattern, symmetry breaking takes away (or renders invisible) $\lceil \sigma_{break} I_\Sigma \rceil$ pellets.

Color symmetry

Using the mathematical concept of algebraic groups and understanding symmetry as a mapping that preserves certain structures, the notion of symmetry can be expanded beyond solely accounting for isometries of geometric aspects, for instance towards color symmetry or dilation (Liu et al., 2010; Weyl, 1952). For the sand-bubbler patterns specified by Eq. (1), color symmetry appears to be particularly interesting. The patterns found in nature on tropical beaches are typically monochromatic as they have the color of the sand they are built from (and beaches with sand of different colors are rather rare). In the artistic interpretation of sand-bubbler patterns, it was proposed to color the pellets according to the chronological order of the placement, or to give each burrow a specific color. In fact, color is not an intrinsic property of such a pattern, but requires a design of its own. Any coloring scheme thinkable could be applied. Thus, a colored sand-bubbler pattern needs to specify the color c_{ijk} of each pellet location $(x_{ijk}, y_{ijk})^T$. The color may vary over pellets, or trenches, or burrows.

Color symmetry (Schwarzenberger, 1984; Senecha, 1983, 1988) of a pattern means that the coloring of the geometric objects building the pattern is consistent with the symmetry properties of these objects. Suppose there is a symmetry group of a pattern, for instance the isometric symmetries ϕ acting on a pellet according to $(x_{ijk}, y_{ijk})^T \rightarrow \phi(x_{ijk}, y_{ijk})^T$ as defined by Eqs. (2)-(5). Further assume the pellet has the color c_{ijk}. Then color symmetry implies that every ϕ is associated with a color permutation giving the symmetric pellet the color $\theta(c_{ijk})$. The mapping from symmetry ϕ to color permutation θ is homomorphic. Put differently, the symmetry properties of the geometric objects define consistently the coloring of these objects. The colors can be specified by a permutation group of colors, while the color permutation can be realized by a mapping on a color wheel. Based on this understanding, breaking color symmetry of a pattern can be achieved similarly to the symmetry breaking of the geometric aspects of patterns as described above. We again set the number of pellets for which color symmetry breaking applies by σ_{break}. A broken color symmetry means that for these pellets the color is not determined by the color permutation of the “unbroken” pellets, but is either produced by a different permutation or defined otherwise. The computational experiments reported next also deal with color symmetry. To distinguish between pattern symmetry breaking and color symmetry breaking, we call $\sigma_{break}(p)$ the pattern symmetry breaking rate and $\sigma_{break}(c)$ the color symmetry breaking rate.

Computational experiments and results

Creating images with symmetry and broken symmetry

For illustrating the effect of the different symmetries and symmetry breaking schemes discussed in the section above,

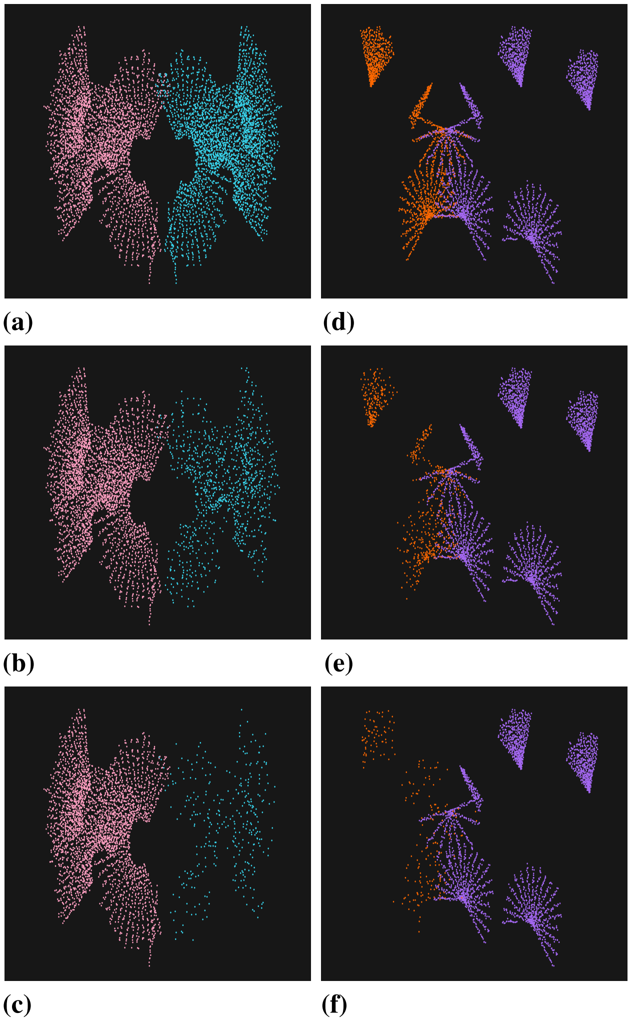

Figure 1: Images with dichromatic symmetry generated by reflection and translation with different symmetry breaking rates. Upper panels **(a)**, **(d)**: $\sigma_{break}(p) = 0$, middle panels **(b)**, **(e)**: $\sigma_{break}(p) = 0.1$, lower panels **(c)**, **(f)**: $\sigma_{break}(p) = 0.3$.

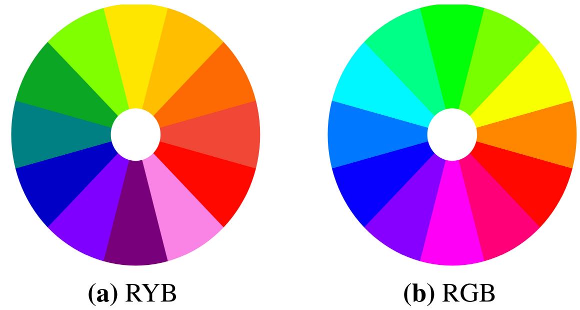

Figure 2: A RYB (red-yellow-blue) **(a)** and a RGB (red-green-blue) **(b)** color wheel with 12 slots, which are used to build color permutation groups with degree up to 12

we consider some examples. We start with pattern symmetry, see Fig. 1 showing dichromatic images. In principle, and if the background has a color different from the pellets and is not counted, displaying symmetry could also be possible in monochromatic images, for instance black (or white) on a white (or black) background. Nevertheless, from an artistic as well as from a computational point of view, dichromatic and polychromanic symmetry appears to be more interesting as it opens up to experiment with color symmetry as well.

The upper left and right images (Fig. 1**(a)** and 1**(d)** show full symmetry by reflection, while in the right image there is additionally a translation. The other panels depict the same image with different degrees of symmetry breaking. In the left panels (Fig. 1**(b)** and 1**(c)** the symmetry breaking is achieved by removing (or making invisible) pellets, while in the right panels (Fig. 1**(e)** and 1**(f)** only the reflected pellets undergo symmetry breaking and are additionally moved by realizations of a random variable. We see that the symmetry by reflection fades for the symmetry breaking rate getting larger, up to the point where it cannot be recognized anymore.

The images in Fig. 1 not only represent pattern symmetry, but also a simple form of color symmetry. Color symmetry depends on the context of geometric symmetry of a (possibly monochromatic) pattern to induce a permutation of colors. This permutation of colors needs to be consistent with the geometric symmetry insofar as some (or all) symmetry operations change the colors, while some other operations (or none) preserve color. For dichromatic images as in Fig. 1 the color permutation group has degree 2, which is to say there are only 2 colors. We see in the images that the pattern symmetry leads to a color change if the symmetry is by reflection and preserves the color if the symmetry is by translation, which is a simple form of color symmetry. To obtain a polychromatic color symmetry we need a permutation group of degree N, with N the number of colors involved. Such a color permutation can be realized by a mapping on a color wheel with N slots, see the example of a RYB and a RGB color wheel, both with 12 slots, in Fig. 2. A broken color symmetry implies that not all pellets experience the color permutation, but a fraction only. In other words, we perturb the change-or-preserve-color arrangement induced by the color permutation.

Fig. 3 shows such a color symmetry and also the results of some experiments with color symmetry breaking. The color permutation is realized using a RYB (red-yellow-blue) color wheel (Itten, 1973; Rhyne, 2017), see Fig. 2**(a)**. It is commonly called the standard artistic color wheel and defines 3 primary colors: **r**ed, **y**ellow and **b**lue. Mixing 2 of these colors each gives the 3 secondary colors: **o**range (red and yellow), **p**urple (red and blue) and **g**reen (yellow and blue). From these 3 primary and 3 secondary colors, another 6 tertiary colors can be derived by mixing: **ve**rmilion (red and

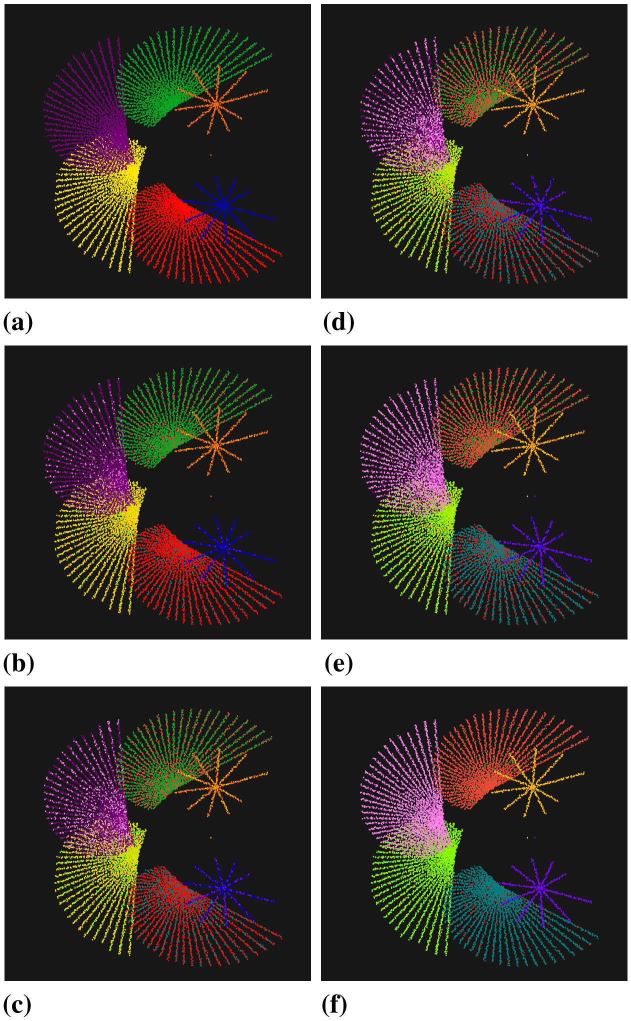

Figure 3: Images with polychromatic symmetry using a RYB color wheel generated by rotation with varying rotation center points and different color symmetry breaking rates. From upper left panel to lower right panel, **(a)**-**(f)**: $\sigma_{break}(c) = (0, 0.15, 0.35, 0.55, 0.75, 0.95)$.

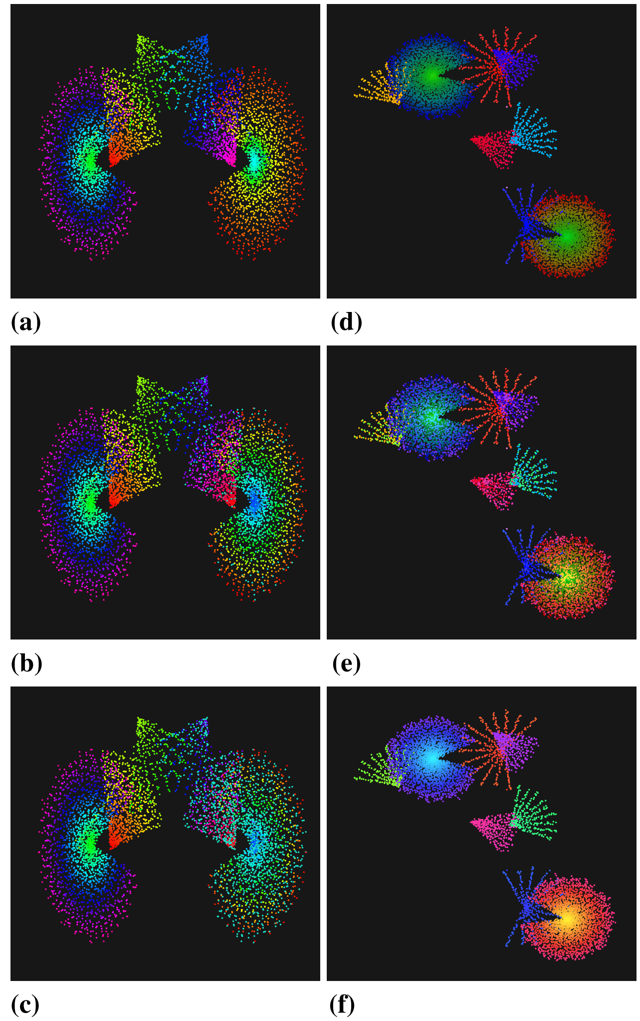

Figure 4: Images with polychromatic symmetry using a RYB and a RGB color wheel generated with different color symmetry breaking rates. Left panels from top to bottom, **(a)**-**(c)**: $\sigma_{break}(c) = (0, 0.25, 0.75)$, right panels top to bottom **(d)**-**(f)**: $\sigma_{break}(c) = (0, 0.50, 0.95)$.

orange), **am**ber (orange and yellow), **ch**artreuse (yellow and green), **te**al (green and blue), **vi**olet (blue and purple) and **ma**genta (purple and red). Fig. 3**(a)** shows an image with full color symmetry. The pattern consists of 3 burrows that each have a symmetric counterpart. Thus, there are 6 burrows in total. The 3 burrows in the lower half of the image are colored with the 3 primary colors according to the RYB color wheel. The symmetric burrows in the upper half of the image are colored with the secondary colors so that the symmetry of the pattern yields the complementary color of the RYB wheel, which is the color exactly opposite on the wheel, see Fig. 2**(a)**. Accordingly, red and green, yellow and purple, and blue and orange are complementary colors. Using Cauchy's two-line notation for describing the color permutation group, we can write $\theta = \begin{pmatrix} \mathbf{r} & \mathbf{y} & \mathbf{b} \\ \mathbf{g} & \mathbf{p} & \mathbf{o} \end{pmatrix}$ to express this color symmetry. We now break the color symmetry. Therefore, a fraction of pellets is selected at random with the symmetry breaking rate $\sigma_{break}(c)$ and colored with tertiary colors according to the RYB wheel. In other words, we break the color symmetry between red and green by perturbing red with chartreuse and green with magenta, and the color symmetry between yellow and purple by perturbing with teal and vermilion, and so on. In some sense, this example of color symmetry breaking finally yields another full symmetry for $\sigma_{break}(c) = 1$, for which there is another color permutation group, $\theta' = \begin{pmatrix} \mathbf{ch} & \mathbf{te} & \mathbf{vi} \\ \mathbf{ma} & \mathbf{ve} & \mathbf{am} \end{pmatrix}$ in two-line notation. The results shown in Fig. 3**(b)**-**(f)** are the intermediate steps between two unbroken color symmetries. The color symmetry breaking shown in the panels are specified by each color element of θ perturbing the corresponding color element of θ', and vice versa.

The next experiment involves a RGB (red-green-blue) color wheel, which is based on the light model of color and commonly finds usage in computer graphics (Rhyne, 2017; Shevell, 2003), see Fig. 2(**b**). Although roughly the RGB color wheel covers the same color spectrum as the RYB color wheel, the colors are distributed differently on the wheel. Particularly, the complementary colors (which are placed opposite on the color wheel) are different. In addition, the warmer colors are spread further around on the RYB wheel, which gives the RGB wheel a somewhat cooler appearance. This gives rise to another color symmetry, see Fig. 4. The patterns are obtained by rotation and glide reflection. Fig. 4(**a**) shows a pattern colored by a RGB wheel. In Fig. 4(**b**)-(**c**) there is a broken color symmetry as for the symmetric pattern in the right half of the image fractions of pellets are colored in cyan. In Fig. 4(**d**)-(**f**)) the complete pattern is mapped in two fractions from a RYB color wheel onto a RGB color wheel. This means that the color symmetry is broken by perturbing the color of the RYB slots with the color of the RGB slots for each slot with the same position on the color wheel according to Fig. 2. For instance, green perturbs yellow, or cyan perturbs green, and so on. According to the distribution of warm colors on the color wheels, the lower image should appear somewhat cooler than the upper image. Looking at Fig. 4(**d**)-(**f**)), it is in the eye of the beholder, of course, to appreciate the effect.

Analysis by a symmetry measure

A further aim of this paper is to analyze how a computational metric may identify symmetry and symmetry breaking. As symmetry implies that parts of the image in some ways resemble each other, the main algorithmic approach to symmetry evaluation works by dividing the image and analyzing the parts. One method is to define axis along the diagonals of the image (for instance the horizontal, vertical, main and secondary diagonal) and comparing the sections on opposing sides of the axis (Gartus and Leder, 2017; Liu et al., 2010). Another approach is to partition the image into rectangles of equal size and comparing them. This method has been proposed and studied by den Heijen and Eiben (2012); den Heijen (2015) and involves to partition the image into 4 areas. We apply this method here and extended it by considering a finer partitioning into 16 quadrants.

We compare the areas by evaluating the differences in intensity for each RGB pixel. In the experiments, we consider the images to have 256×256 pixels. The intensity $I_n(i,j)$ of a pixel (ij) belonging to an area A_n is obtained as the average of its red (R), green (G) and blue (B) value: $I_n(i,j) = (R(i,j) + G(i,j) + B(i,j))/3$. Thus, the similarity between a pixel (i,j) belonging to the area A_n and a pixel (i,j) belonging to the area A_m is

A_{11}	A_{12}	A_{13}	A_{14}
A_{21}	A_{22}	A_{23}	A_{24}
A_{31}	A_{32}	A_{33}	A_{34}
A_{41}	A_{42}	A_{43}	A_{44}

Figure 5: Calculating of the symmetry measure

$$sim(A_{n_{i,j}}, A_{m_{i,j}}) = \begin{cases} 1 & \text{if } |I_n(i,j) - I_m(i,j)| < \alpha, \\ 0 & \text{otherwise} \end{cases}$$

with α a difference threshold. In the experiments, there is $\alpha = 0.05$ (and $0 \leq I_n \leq 1$). For similarity of whole areas we average over all pixels:

$$sim(A_n, A_m) = \frac{1}{\mathcal{I}\mathcal{J}} \sum_{i=1}^{\mathcal{I}} \sum_{j=1}^{\mathcal{J}} sim(A_{n_{i,j}}, A_{m_{i,j}}),$$

where $\mathcal{I}$ and $\mathcal{J}$ are the number of pixels in the (x,y)-plane, with $\mathcal{I} = \mathcal{J} = 256$ in the experiments reported here. We define a **l**eft area by $A_{\mathbf{l}} = A_{11} \cup A_{21} \cup A_{31} \cup A_{41}$, a **m**iddle **l**eft by $A_{\mathbf{m\,l}} = A_{12} \cup A_{22} \cup A_{32} \cup A_{42}$, a **m**iddle **r**ight by $A_{\mathbf{m\,r}} = A_{13} \cup A_{23} \cup A_{33} \cup A_{43}$ and a **r**ight area by $A_{\mathbf{r}} = A_{14} \cup A_{24} \cup A_{34} \cup A_{44}$, see Fig. 5. The same is done likewise for vertical areas: **t**op, **m**iddle **t**op, **m**iddle **b**ottom and **b**ottom. For the horizontal symmetry sym_h we calculate the average similarity between the left and the areas to the right

$$sym_h = (sim(A_{\mathbf{l}}, A_{\mathbf{r}}) + sim(A_{\mathbf{l}}, A_{\mathbf{m\,l}}) + sim(A_{\mathbf{l}}, A_{\mathbf{m\,r}}))/3,$$

while for the vertical symmetry sym_v, we take likewise into account the averaged similarities between the top and the areas below: $sim(A_{\mathbf{t}}, A_{\mathbf{b}})$, $sim(A_{\mathbf{t}}, A_{\mathbf{m\,t}})$ and $sim(A_{\mathbf{t}}, A_{\mathbf{m\,b}})$. The comparison of areas by sym_h and sym_v can be seen as a generalized form of relating left-to-right and top-to-bottom. It does not presume a symmetry axis along the horizontal and vertical central axis as for instance would have been imposed by $(sim(A_{\mathbf{l}}, A_{\mathbf{r}}) + sim(A_{\mathbf{m\,l}}, A_{\mathbf{m\,r}}))/2$ or $(sim(A_{\mathbf{t}}, A_{\mathbf{b}}) + sim(A_{\mathbf{m\,t}}, A_{\mathbf{m\,b}}))/2$. However, by this comparison of areas a bias is introduced towards the left and top of the image. Additional experiments (not depicted in the figures) have shown that the results are qualitatively the same if the bias is towards the right or the bottom. This appears to be plausible as the images have no natural orientation.

The symmetry measure SYM taking into account a partition into 16 areas of the image as shown in Fig. 5 is the average over the two symmetries:

$$\text{SYM} = (sym_h + sym_v)/2. \tag{6}$$

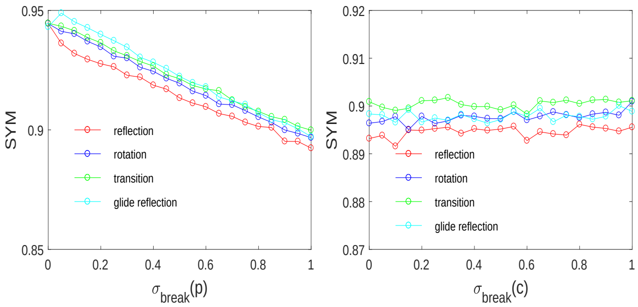

(a) **(b)**

Figure 6: The symmetry measure SYM as a function of the symmetry breaking rates σ_{break} for both symmetry breaking of pattern and color symmetry breaking

Fig. 6 shows the results of computational experiments with symmetry and symmetry breaking in digitally generated artificial-life-based visual art. The symmetry measure SYM is shown as a function of the symmetry breaking rates σ_{break} for symmetry breaking of both pattern and color. The results are for 21 equidistant values of the symmetry breaking rate σ_{break} with $0 \leq \sigma_{break} \leq 1$.

For each value of σ_{break}, 2000 images with patterns were generated according to the algorithmic framework described above. Each image is different as some of the algorithm's parameters depend on realizations of a random process. For analyzing the effect of symmetry breaking the color of each pellet is assigned at random. This is done by coloring each pellet with a realization of a random variable uniformly distributed on the RGB color space. Symmetry breaking of the pattern is done by pellets being removed (or made invisible). Looking at the results, we see that for pattern symmetry (Fig. 6(**a**)) the symmetry measures fall almost linearly with the symmetry breaking rate $\sigma_{break}(p)$. For $\sigma_{break}(p) = 0$, where the symmetry is completely intact, we have the highest values of SYM. The values fall for $\sigma_{break}(p)$ getting larger and are smallest for $\sigma_{break}(p) = 1$, where symmetry generated by the isometric maps is completely gone. However, we also see that the values of the symmetry measures for $\sigma_{break}(p) = 1$ are not really small. We find SYM ≈ 0.9. This can be explained by even a single sand-bubbler pattern displaying a considerable degree of symmetry. Look, for instance, at the pattern on the left-hand side of Fig. 1(**a**). Here, the trenches of the pattern form hands around the center point for more than a semicircle. Thus, there is symmetry in itself, and the symmetry measure SYM accounts for it. However, generating additional symmetry by the isometric maps (2)-(5) increases the value of the symmetry measure even more, which shows its ability to identify different shades of symmetry. A further result is that the symmetry measure enables differentiating between the different types of symmetry, with reflection (2) giving slightly smaller values than rotation (3), transition (4) and glide reflection (5).

The curves for color symmetry breaking are shown in Fig. 6(**b**). Symmetry breaking of colors is done by shifting the colors of the selected pellets randomly through the RGB color space. The results show that a higher degree of symmetry breaking (that is, a higher percentage of pellets that change their color) does not give very different values of the symmetry measures. In fact, SYM slightly drifts but has essentially the same value for all $0 \leq \sigma_{break}(c) \leq 1$. This is a consequence of how the symmetry measure is calculated. For a given collection of pellets it accounts for differences in the spatial distribution of their average RGB values. Thus, a random shift through the RGB color space does not systematically alter intensity. Such an alteration can be achieved if breaking the color symmetry has a bias towards one of the RGB components. Experiments indeed show this to be the case. However, such a bias is completely arbitrary and does not make the symmetry measure truly able to quantify color symmetry breaking. Finally, it can be observed that for color symmetry breaking (as for pattern symmetry breaking) SYM allows to differentiate between types of symmetry.

It may finally be interesting to note that a coarser or finer grid of areas deteriorates the results. Additional experiments with 4 and 64 areas (not shown in figures due to brevity) have shown that the curves for the isometric maps (2)-(5) lump together. This immediately suggests the conjecture that there is a grid optimal for differentiating between types of symmetry, which may depend on the granularity of the pellets. This appears understandable as the pellets have a finite size, which is relative to the size of the image. The pellets have no structure on every scale as for instance have fractals, which is the main reason for fractal dimensions not being useful for evaluating the images considered in this paper.

Concluding remarks

In this paper symmetry and symmetry breaking in digitally generated artificial-life-based visual art is discussed. Its main focus is on concepts and templates for incorporating symmetry and broken symmetry into the creation process of bioinspired art. Using the example of sand-bubbler patterns as a test bed, all four types of isometric symmetry in two-dimensional space are employed. In addition, also color symmetry is considered and realized as a color permutation consistent with the isometric maps. Therefore, color permutation groups have been designed which utilize mappings on a color wheel.

In more abstract terms symmetry has been described as "immunity to a possible change," (Rosen, 1995). Such an understanding, however, may also suggest the interpretation that symmetry implies redundancy (or even the absence of novelty). This has been the main motivation to explore intermediate states between complete symmetry in a mathematical sense and no symmetry at all, which have been treated as symmetry breaking. The artistic interpretation proposed in this paper is that broken symmetry means that certain parts (or aspects) of symmetry become invisible as a result of the symmetry breaking process. It is also shown that a computational symmetry measure is able to identify different types of symmetry and symmetry breaking in the images.

The visual and analytic results presented in the paper only cover a small subset of possible designs. Thus, future work could focus on exploring the design space to a larger extent. For instance, the color permutations discussed in connection with color symmetry only considered hue, but could also include saturation or lightness. Furthermore, whole patterns could be used as a motif or building block to create more complex patterns, for instance by combining or repeating isometric maps. Thus, by employing the concept of wallpaper or frieze groups (Coxeter, 1986; Conway et al., 2008; Thomas, 2012) images could be produced that broaden the spatial scope.

References

Adanova, V., Tari, S. (2016). Beyond symmetry groups: A grouping study on Escher's Euclidean ornaments. *Graphical Models* 83, 15–27.

Abbood, Z. A., Amlal, O., Vidal, F. P. (2017). Evolutionary art using the fly algorithm. In: Squillero, G., Sim, K. (eds.) *Applications of Evolutionary Computation. EvoApplications 2017*, pages 455–470, Springer, Cham.

al-Rifaie, M. M., Ursyn, A., Zimmer, R., Javid, M. A. J. (2017). On symmetry, aesthetics and quantifying symmetrical complexity. In: Correia J., et al. (eds) *Computational Intelligence in Music, Sound, Art and Design. EvoMUSART 2017*, pages 17–32, Springer, Cham.

Ball, P. (2009). *Shapes. Nature's Patterns: A Tapestry in Three Parts.* Oxford University Press, Oxford.

Bier, C. (2001). Mathematical aspects of oriental carpets. *Symmetry Sci. Culture (Budapest)* 12, 67–77.

Bier, C. (2005). Symmetry and symmetry–breaking: An approach to understanding beauty. In: Sarhangi, R., Moody, R. V. (eds) *Renaissance Banff: Mathematics, Music, Art, Culture*, pages 219–226, Bridges, Winfield, KA.

Boden, M. A. (2015). Creativity and ALife. *Artificial Life* 21, 354–365.

Conway, J. H., Burgiel, H., Goodman-Strauss, C. (2008). *The Symmetries of Things.* A K Peters, Wellesley, MA.

Coxeter, H. S. M. (1986). Coloured symmetry. In: Coxeter, H. S. M., Emmer, M., Penrose, R., Teuber, M. L. (eds) *M.C. Escher: Art and Science*, pages 15–33, North–Holland, Amsterdam.

den Heijer, E., Eiben, A. E. (2014). Investigating aesthetic measures for unsupervised evolutionary art. *Swarm Evol. Comput.* 16, 52–68.

den Heijer, E. (2015). Evolving symmetric and balanced art. In: Madani K., et al. (eds) *Computational Intelligence*, pages 33–47, Springer, Cham.

Dunham, D. (2010). Creating repeating patterns with color symmetry. In: Akleman, E., Friedman, N. (eds), *Proc. ISAMA 2010 Conf.*, pages 7–14, De Paul University, Chicago, IL.

Galanter, P. (2016). Generative art theory. In: Paul, C. (ed.) *A Companion to Digital Art*, pages 146–180, John Wiley, Chichester.

Gartus, A, Leder, H. (2017) Predicting perceived visual complexity of abstract patterns using computational measures: The influence of mirror symmetry on complexity perception. *PLoS ONE* 12(11), e0185276.

Greenfield, G., Machado, P. (2015). Ant– and ant–colony–inspired Alife visual art. *Artificial Life* 21, 293–306.

Grünbaum, B., Grünbaum, Z., Shepard, G. C. (1986). Symmetry in Moorish and other ornaments. *Comp. Math. Appl.* 12, 641–653.

Itten, J. (1973). *The Art of Color: The Subjective Experience and Objective Rationale of Color.* Van Nostrand Reinhold, New York.

Jacob, C. J., Hushlak, G., Boyd, J. E., Nuytten, P., Sayles, M., Pilat, M. (2007). Swarmart: Interactive art from swarm intelligence. *Leonardo* 40, 248–254.

Liu, Y., Hel–Or, H., Kaplan, C. S., Van Gool, L. (2010). Computational symmetry in computer vision and computer graphics. *Foundations and Trends in Computer Graphics and Vision 5: 1–2*, 1–195.

Martin, G. E. (1982). *Transformation Geometry: An Introduction to Symmetry.* Springer, New York.

Molnar, V., Molnar, F. (1986). Symmetry–making and –breaking in visual art. *Comp. Math. Appl.* 12, 291–301.

Ouyang, P., Cheng, D., Cao, Y., Zhan, X. (2012). The visualization of hyperbolic patterns from invariant mapping method. *Computers & Graphics* 36, 92–100.

Richter, H. (2018). Visual art inspired by the collective feeding behavior of sand–bubbler crabs. In: Liapis A., et al. (eds) *Computational Intelligence in Music, Sound, Art and Design. EvoMUSART 2018*, pages 1–17, Springer, Cham.

Rosen, J. (1995). *Symmetry in Science*. Springer, New York.

Rosen, J. (2009). *Symmetry Rules: How Science and Nature are Founded on Symmetry*. Springer, New York.

Romero, J., Machado, P. (eds.) (2008). *The Art of Artificial Evolution: A Handbook on Evolutionary Art and Music.* Springer, New York.

Rhyne, T. M. (2017). *Applying Color Theory to Digital Media and Visualization.* CRC Press, Boca Raton, FL.

Schattschneider, D. (2004). *M.C. Escher: Visions of Symmetry.* Thames & Hudson, London.

Schattschneider, D. (2017). Lessons in duality and symmetry from M.C. Escher. In: Fenyvesi K., Lähdesmäki T. (eds) *Aesthetics of Interdisciplinarity: Art and Mathematics*, pages 105–118, Birkhäuser, Cham.

Schwarzenberger, R. L. E. (1984). Colour symmetry. *Bull. London Math. Soc.* 16, 209–240.

Senechal, M. (1983). Coloring symmetrical objects symmetrically. *Math. Magazine* 56, 3–16.

Senechal, M. (1988). Color Symmetry. *Comp. Math. Appl.* 16, 545–553.

Shevell, S. K. (2003). *The Science of Color*. Elsevier, Amsterdam.

Shubnikov, A. V., Koptsik, V. A. (1974). *Symmetry in Science and Art*. Plenum Press, New York.

Thomas, B. G. (2012). Colour symmetry: the systematic coloration of patterns and tilings. In: Best, J. (ed) *Colour Design – Theories and Applications*, pages 381–432, Woodhead Publishing, Cambridge, UK.

Thompson, D'Arcy W. (1942). *On Growth and Form, 2nd Edition.* Cambridge University Press, Cambridge, UK.

Urbano, P. (2011). The *T. albipennis* sand painting artists. In: Di Chio, C., et al. (eds) *Applications of Evolutionary Computation. EvoApplications 2011*, pages 414–423, Springer, Berlin.

Weyl, H. (1952). *Symmetry.* Princeton University Press, Princeton, NJ.

Whitelaw, M. (2004). *Metacreation. Art and Artificial Life.* MIT Press, Cambridge, MA.